Isolation and characterization of novel phages targeting pathogenic *Klebsiella pneumoniae*

Na Li[1#], Yigang Zeng[2#], Rong Bao[1], Tongyu Zhu[1], Demeng Tan[2*], Bijie Hu[1*],

[1]Zhongshan Hospital, Fudan University, Shanghai, China

[2]Shanghai Public Health Clinical Center, Fudan University, Shanghai, China

[#]These authors contributed equally: Na Li, Yigang Zeng

***Correspondence: Demeng Tan (demengtan@gmail.com) and Bijie Hu (hu.bijie@zs-hospital.sh.cn)**

Abstract

Klebsiella pneumoniae is a dominant cause of community-acquired and nosocomial infections, specifically among immunocompromised individuals. The increasing occurrence of multidrug-resistant (MDR) isolates has significantly impacted the effectiveness of antimicrobial agents. As antibiotic resistance is becoming prevalent, the use of bacteriophages to treat pathogenic bacterial infections is becoming revitalized. Elucidating the details of phage-bacteria interactions will provide insights into phage biology and the better development of phage therapies. In this study, a total of 22 *K. pneumoniae* isolates were assessed for their genetic and phenotypic relatedness by multi-locus sequence typing (MLST), endonuclease S1 nuclease pulsed-field gel electrophoresis (S1-PFGE), and *in vitro* antibiotic susceptibility testing. In addition, the beta-lactamase gene (bla_{KPC}) was characterized to determine the spread and outbreak of *K. pneumoniae* carbapenemase (KPC)-producing enterobacterial pathogens. Using these *K. pneumoniae* isolates, three phages were isolated and characterized to evaluate the application of lytic phages against these 22 ST11 *K. pneumoniae* isolates. *In vitro* inhibition assays with three phages and *K. pneumoniae* strain ZS15 demonstrated the strong lytic potential of the phages, however, followed by the rapid growth of phage-resistant mutants. Together, this data adds more comprehensive knowledge to known phage biology and further emphasizes their complexity and future challenges to overcome prior to using phages for controlling this important MDR bacterium.

Keywords: Bacteriophage; Phage therapy; *Klebsiella pneumoniae*; Phage-host interactions; Multidrug-resistance

43 **Introduction**

44 The ongoing explosion of the antimicrobial resistance crisis has been accelerated by the
45 overuse and misuse of antibiotics, causing the emergence and increased prevalence of
46 MDR bacteria (Ventola, 2015). *Klebsiella pneumoniae*, a Gram-negative
47 *Enterobacterales*, can be found in the environment and has been associated with
48 community-acquired infections (Pendleton et al., 2013). The increasingly common
49 mechanism of carbapenem resistance in *K. pneumoniae* is mediated by extended-
50 spectrum β-lactamases (ESBLs), which are able to break the β-lactam structure in the
51 most commonly used antibiotics (Pitout et al., 1997). Thus, infections of KPC-producing
52 bacteria are consistently associated with poor clinical outcomes and represent a
53 significant and continued threat to the healthcare system. As this problem continues to
54 grow, there is a strong need to find an alternative means to conventional antimicrobials
55 in order to combat this clinical pathogen.

56 Bacteriophages (phages for short) are the most common and diverse biological entities
57 in the biosphere, playing an important role in promoting bacterial diversity, structuring
58 community composition, and being a key driver in nutrient turnover (Suttle, 2005). Lytic
59 phages infect and lyse bacterial hosts and are an attractive alternative towards
60 combating the fast development of antibiotic-resistant *K. pneumoniae* (Sulakvelidze et
61 al., 2001;Hung et al., 2011). The use of phages has gained interest over the past years
62 and phages that are specific for MDR bacterial pathogens, including *Pseudomonas*
63 *aeruginosa*, *Enterococcus* spp., *Mycobacterium abscessus*, *Staphylococcus aureus*, *A.*
64 *baumannii*, and *Escherichia coli* have been identified and used to treat bacterial

65 infections (Chibani-Chennoufi et al., 2004b;Capparelli et al., 2007;McVay et al.,
66 2007;Letkiewicz et al., 2009;Schooley et al., 2017;Abd El-Aziz et al., 2019;Dedrick et al.,
67 2019;Cano et al., 2020). These studies demonstrated that lytic phages can be harnessed
68 to prevent and eradicate pathogenic bacteria, and in some cases, alleviate current
69 medical challenges posed by antibacterial resistance and thus further reduce
70 mortalities. While previous applications of phage therapy have shown promising results,
71 the technology is still in a stage of development due to rapid evolution dynamics
72 between phages and their hosts (Chibani-Chennoufi et al., 2004a). It is, therefore,
73 crucial to characterize both phage and host communities prior to any intended phage
74 applications.

75 In this study, we analyzed the molecular epidemiological feature of a collection of 22
76 clinical *K. pneumoniae* isolates, specifically on the characteristics of MLST, plasmid, and
77 antibiotic susceptibility patterns. Using these *K. pneumoniae* isolates, we isolated and
78 characterize three phages native to the hospital sewage. Details of phage host range,
79 genome, morphological characters, and phage-host interactions were established to
80 assess the application of phage therapies against the carbapenem-resistant isolates.
81 Together, our study provides important information regarding the treatment and
82 prevention of this important human pathogen.

83 **Materials and methods**

84 **Bacterial strains and growth conditions**

85 Twenty-two nonduplicate bacterial isolates of *K. pneumoniae* were collected from
86 Zhongshan Hospital, Shanghai, China and identified with MALDI-TOF Mass Spectrometry
87 (Bruker, USA) from June 2019 - May 2020. Isolates were routinely grown in either Luria-
88 Bertani broth (LB) containing per liter: tryptophan 10 g, NaCl 10 g, and Yeast extract 5 g
89 with aeration, or, on LB agar (15 g agar per liter) plates at 37°C. The beta-lactamase
90 gene (bla_{KPC}) was detected by PCR Master Mix (Thermo, CA, USA) with forward primer
91 5'-TGTAAGTTACCGCGCTGAGG-3' and reverse primer 5'-CCAGACGACGGCATAGTCAT-3'.
92 All strains were stored at -80°C in LB broth with 25% glycerol (vol/vol) and sub-
93 cultivated before each use.

94 **Multi-locus sequence typing (MLST) and antibiotic susceptibility of bacterial isolates**

95 In order to study population genetics and micro-evolution of this epidemic bacteria,
96 MLST was applied to characterize these 22 isolates using sequences of internal
97 fragments of seven house-keeping genes, according to the protocol available on the
98 MLST Pasteur website (https://bigsdb.pasteur.fr/klebsiella/klebsiella.html) (Diancourt et
99 al., 2005). The purified MLST amplicons were sent for Sanger sequencing, followed by
100 further comparison with those available on the MLST database to determine the
101 sequence type (ST). The VITEK2 compact automated system (bioMérieux, Lyon, France)
102 was used to determine antibiotic susceptibility profiles according to the manufacturer's
103 instructions. The susceptibility breakpoints were interpreted with reference to the latest
104 documents from the Clinical and Laboratory Standards Institute (CLSI).

105 **S1-Pulsed Field Gel Electrophoresis (S1-PFGE)**

106 *Klebsiella* with plasmid-mediated carbapenem resistance poses significant challenges in
107 clinical practice. To characterize the plasmid content in each strain, S1 nuclease
108 digestion analyzed with PFGE was performed using a CHEF Mapper XA apparatus (Bio-
109 Rad Laboratories, Hercules, CA). Briefly, the adjusted bacterial suspension mixed in a 1%
110 agarose gel was digested with a proteinase K solution for 2 h at 54°C, then further
111 treated with S1 nuclease. The electrophoresis conditions used in this study were as
112 follows: initial switch time, 3 s; a final switch time, 36 s; gradient, 6 V/cm; angle, 120;
113 temperature, 14°C; and time, 18.5 h. After the electrophoresis run was complete, the
114 gel was stained with 1 mg/mL ethidium bromide and visualized with the ChemiDoc XRS
115 system (Bio-Rad Laboratories, CA, USA). Genetic similarities were measured using the
116 Dice coefficient and the clustering was carried out by the unweighted-pair group
117 method with arithmetic averages (UPGMA) in BioNumerics (Applied Maths).

118 **Isolation and proliferation of phage**

119 Phages were isolated using an enrichment protocol as described previously (Tan et al.,
120 2014). Briefly, infiltrated hospital sewage was mixed with the same volume of 2 × LB
121 broth and incubated at 37°C for 6 h to stimulate proliferation of total abundances of
122 specific phages targeting the *K. pneumoniae* isolates above. Aliquots of enrichment
123 samples were centrifuged (12,000×*g*, 10 min, 4°C) and sterilized with 0.1% chloroform.
124 The presence of *K. pneumoniae*-phages in the hospital sewage samples was detected by
125 double-layer agar assays with different fold dilutions of the cell-free spent supernatant
126 from the enrichment assay. In order to obtain individual phages, single plaques were

127 picked and purified three times with their corresponding hosts. Phage stocks were
128 enriched and titrated using double-layer agar assays as described previously and stored
129 at 4°C before use (Kropinski et al., 2009).

130 **Phage-host range assay**

131 The host range of obtained phages was determined against 22 clinical isolates by
132 standard spot assays. Aliquots of 2 µL diluted phage lysate (~10^5 PFU ml^{-1}) was spotted
133 on lawns containing 4 mL top agar mixed with 300 µL mid-log phase bacteria. After
134 incubating at 37°C for 12 h, the spots were assessed by the turbidity of plaques and
135 characterized as strong infection (clear), weak infection (turbid), or no inhibition (no
136 plaque). The experiment was undertaken as independent duplicates.

137 **Susceptibility of strain ZS15 to phage infection and isolation of phage-resistant**
138 **mutants**

139 Overnight bacterial cultures were 1,000-fold diluted into LB broth and grown to an
140 exponential phase with an OD600 at 0.3 and infected with its corresponding phages at
141 an multiplicity Of infection (MOI) of 0.01. The suspension was incubated at 37°C with
142 aeration and samples were harvested at 1-h intervals. The phage lysis efficiency was
143 determined by optical density measurements. The experiment was done in triplicate
144 along with parallel control cultures without phages. At time point 8-h, phage lysates
145 were streaked onto LB agar plates and individual colonies were subsequentially purified
146 to determine phage susceptibility by spot test assays as described above.

147 **Phage DNA extraction and genomic analysis**

148 For the extraction of phage DNA, 2 mL aliquots of phage lysate with a titer of
149 approximately 10^9 PFU mL^{-1} was digested with DNase I (Thermo, CA, USA) and RNase A
150 (Promega, USA) to remove any residual bacterial genomic DNA and RNA according to
151 the manufacturer's protocol. After digesting for 1.5 h at 37°C, EDTA (Thermo, CA, USA)
152 was added to a final concentration of 20 mM to inactivate DNase I and RNase A. Total
153 phage DNA was extracted using the Qiagen DNeasy Blood and Tissue kit (Qiagen, CA,
154 USA) following the manufacturer's instructions. Genomic DNA was sent to Sangon
155 Biotech (Shanghai, China) and sequenced using an Illumina HiSeq sequencer.

156 The raw sequence containing the phage genome was quality controlled and trimmed
157 with FastQC 0.11.2 (https://www.bioinformatics.babraham.ac.uk/projects/fastqc/) and
158 Trimmomatic 0.36 (http://www.usadellab.org/cms/?page=trimmomatic). The trimmed
159 reads were assembled into a single raw contig via SPAdes 3.5.0.
160 (http://cab.spbu.ru/software/spades/). Genes were predicted and annotated using
161 Rapid Annotation using Subsystem Technology (RAST, http://rast.nmpdr.org/). Phage
162 virulence factor was examined using Virulence Factor Database (VFDB,
163 http://www.mgc.ac.cn/VFs/). Phylogenetic relationship between the genome of phage
164 NL_ZS_1, NL_ZS_2, and NL_ZS_3 and the genomes of related phages were analyzed
165 using CLC Main Workbench (CLC, Qiagen). To construct the phylogenetic tree of phage
166 terminase large subunits, the reference amino acid sequences of were collected from
167 the NCBI database. The terminase large subunits were aligned, and neighbor-joining
168 tree were created using Jukes-Cantor model with a bootstrap analysis of 1000
169 replicates.

170 **Bacteriophage morphology by TEM**

171 Based on the genomic differences, phages were selected for examination by
172 transmission electron microscopy (TEM). Phage stocks were back-diluted in a SM buffer
173 (50 mM Tris-Cl, pH 7.5, 99 mM NaCl, 8 mM $MgSO_4$, 0.01% gelatin) to a titer of 10^8
174 PFU/mL. Diluted phage lysates were then placed on the surface of Formvar carbon-
175 coated grids (Sigma-Aldrich, St. Louis, MO, USA) for 5 min to allow adsorption. Grids
176 were stained with 2% sodium phosphotungstate for 2 min prior to being washed in a
177 drop of distilled water and air-dried before being examined using a JEM-2100
178 microscope operated at 80 kV.

179 **Results**

180 **Isolation and characterization of *K. pneumoniae* strains**

181 The emergence of carbapenem-resistant *K. pneumoniae* (CRKP) has become one major
182 burden of healthcare-associated infection due to the dispersion of bacteria carrying the
183 bla_{KPC} gene (Bush and Bradford, 2016). KPC was first found in carbapenem-resistant *K.*
184 *pneumoniae* strains in 2001 in North America, and now KPC-producing strains can be
185 frequently isolated from nosocomial samples. It is, therefore, essential to determine and
186 characterize the nosocomial spread of KPC clones and their corresponding phenotype
187 and genotype. Together, 22 *K. pneumoniae* strains were recovered from various clinical
188 specimens. According to the *K. pneumoniae* MLST database, all of the 22 clinical isolates
189 belonged to ST11 (allelic profile 3311114), which is the predominant clone of KPC-
190 producing *K. pneumoniae* in China (Table 1). Despite more than 100 different sequence

191 types (STs) being reported worldwide, the mass dissemination of carbapenemase-
192 producing *K. pneumoniae* has been restricted largely to ST258, ST11, ST340, and ST512
193 (Pitout et al., 2015).

194 In addition, the bla_{KPC} gene was detected in 19 out of 22 isolates, indicating the
195 prevalence of β-lactamase nosocomial pathogens (Table 1). The bla_{KPC} gene can be
196 disseminated between species by horizontal (lateral) gene transfer (HGT) via various
197 means, such as plasmids, transposons, prophages, and integrative conjugative elements
198 (ICEs), which play an important effect in generating genotypic heterogeneity and
199 phenotypic variation among bacterial populations (Hardiman et al., 2016;Botelho and
200 Schulenburg, 2020). For instance, transfer of interspecies KPC can occur through the
201 dissemination of mobile genetic elements between strains of *S. aureus* (Goren et al.,
202 2010).

203 Since pathogenicity and antimicrobial resistance genes are mainly coded by plasmids, in
204 order to identify the subtypes of *K. pneumoniae* ST11, pulsed-field gel electrophoresis
205 with S1 nuclease (S1-PFGE) were utilized to resolve the prevalence of plasmid
206 fingerprints of all the 22 isolates, particularly large ones, which clustered into 6 primary
207 clades (A, B, C, D, E, and F) (Figure 1). Clade A and B were the most common types,
208 while the other clades (C, D, E, and F) accounted for 31.8%. All groups harbored one to
209 two plasmids ranging from 20 Kbp and 250 Kbp. Thus, it appears that S1-PFGE is a highly
210 discriminative molecular typing method capable of effectively discriminating ST11

211 clones into several different subtypes, indicating the prevalence of ST11 was not clonally
212 homogenous.

213 **Imipenem and meropenem resistance involve the production of β-lactamase**

214 Individual antimicrobial data can be found in Table 1. For ticarcillin/clavulanic acid,
215 piperacillin/tazobactam, cefepime, aztreonam, ciprofloxacin, and levofloxacin, drug
216 resistance was detected in all strains. In addition, low percentages of resistance to
217 doxycycline, minocycline, tigecycline, colistin, and trimethoprim/sulfamethoxazole were
218 also observed for most strains. Of these, 17 out of the 22 isolates become resistant to
219 both imipenem and meropenem with a MIC of ≥16 μg/mL, while the other 5 were both
220 sensitive to imipenem and meropenem, except for strain ZS18 which was resistant to
221 imipenem but intermediate to meropenem. For these 5 sensitive isolates, 2 of them
222 were confirmed by PCR and sequencing to have the bla_{KPC} gene. Interestingly, strain ZS4
223 harboring bla_{KPC} was susceptible to imipenem and meropenem, perhaps indicating the
224 resistance is associated with changes in gene expression at the mRNA levels (Senchyna
225 et al., 2019).

226 **Isolation and characterization of phages**

227 Three phages (NL_ZS_1, NL_ZS_2, and NL_ZS_3) were isolated from local hospital
228 sewage using the enrichment protocol to evaluate the potential of phage therapy as an
229 effective alternative against *K. pneumoniae* strains. The host range of the three phages
230 and their lytic efficiency against all of the 22 bacterial isolates were assessed using the
231 spot test assay. According to the host range profile, the phages were able to infect all of

232 the 22 bacterial isolates, however, the phages displayed a unique profile in terms of
233 host range patterns and lytic efficiency (Figure 2). Based on their host susceptibilities,
234 phages were divided into two major groups. Specifically, phage NL_ZS_3 displayed the
235 broadest host range, while phage NL_ZS_1 and phage NL_ZS_2 showed a relatively
236 narrow host range, infecting only ~50% of the tested *K. pneumoniae* strains (Figure 2).
237 The host range differences between the phages observed in this study are very likely
238 due to the different phage characterization, i.e., efficiency of adsorption and lytic
239 efficiency in its potential hosts.

240 **Morphology and genome sequence of phages**

241 All phage lysates formed transparent plaques on strain ZS15, which are considered as an
242 indicator of strong lysis. Plaque morphologies of all phages presented a zone of clear
243 lysis on the host strain ZS15, while a halo zone was detected on the plaques of both
244 phages NL_ZS_1 and NL_ZS_2, indicating the production of polysaccharide
245 depolymerase (Figure 3). Depolymerase activity are usually encoded by their tail fibers
246 or tail spikes protein on the baseplate, which has the potential to provide an alternative
247 treatment to conventional antibiotics.

248 Based on transmission electron microscopy (TEM) analysis, all the phages belong to the
249 family *Podoviridae* of *Caudovirales* order based on the International Committee on
250 Taxonomy of Viruses (ICTV) definitions, having short, non-contractile tails (~11 nm in
251 length) and icosahedral heads (~61 nm diameter) (Figure 3 and Table 2). In addition,
252 total genomic DNA was extracted from each of the three phages, and their genomes

253 were sequenced by Illumina MiSeq. The assembly sizes of these three phages ranged
254 from 38 kb to 40 kb, having a G+C content ranging between 50% to 53%, with 45 to 49
255 predicted protein-coding genes (Table 2). All phage genomes (GenBank accession: phage
256 NL_ZS_1, MT813140; phage NL_ZS_2, MT813141; and phage NL_ZS_3, MT813142) were
257 submitted to RAST (Rapid Annotation using Subsystem Technology) and further
258 annotated by the available pipeline. No identifiable virulent genes, antibiotic resistance
259 genes, or genes involved in lysogenic cycles were detected. Therefore, it appears that
260 those phages isolated in this study can satisfy the safety assessment based on their
261 complete genome sequences. Progressive multiple genome alignments were analyzed
262 using Easyfig software (https://mjsull.github.io/Easyfig/) (Figure 4) to determine the
263 relatedness of three *K. pneumoniae* phages. A considerable relation was shown
264 between phage NL_ZS_1 and phage NL_ZS_2, while phage NL_ZS_2 displays a relatively
265 low homologous region with phage NL_ZS_3. Likely, phylogenetic analysis of the large
266 subunit of the terminase of phage NL_ZS_1, NL_ZS_2, and NL_ZS_3 reveals their close
267 relation to large terminase subunits of other phages, specifically, phage NL_ZS_1 and
268 phage NL_ZS_2 display high similarities to *Klebsiella* phage K11, BIS33, and KpV289,
269 while phage NL_ZS_3 was closely related to *Salmonella* phage phiSG-JL2 (Figure 5).
270 Together, these results showed high relation to the phage-host range pattern,
271 demonstrating phage susceptibility correlates with phage core genome, such as genes
272 involved in the phage tail fibers. However, further studies are needed to probe the
273 genetic determinants that contribute to the host-range difference among these three
274 phage isolates.

275 **Phage growth characteristics in LB broth**

276 To examine the efficiency of phage infection, *K. pneumoniae* ZS15 was infection in liquid
277 cultures with individual phages (NL_ZS_1, NL_ZS_2, and NL_ZS_3) at an MOI of ~0.01,
278 respectively, and their inhibition was assessed by bacterial growth following the
279 measurement of the optical density of the bacterial cultures with and without phages. A
280 similar inhibitory effect of phage NL_ZS_1 and phage NL_ZS_2 was observed in the *in*
281 *vitro* inhibition assay with a drastic decline in optical density on the initial control of the
282 host population for 1.5 h followed by regrowth of the resistant population (Figure 6). A
283 similar trend in the phage-amended cultures of ZS15+ NL_ZS_3 was also observed in the
284 first 5 h, however, it was followed by less pronounced decrease and finally stabilized
285 after 6 h (Figure 6), After 8 h, the OD600 nm of the phage-amended cultures of group 1
286 (ZS15+phage NL_ZS_1 and ZS15+phage NL_ZS_2) and group 2 (ZS15+phage NL_ZS_3)
287 stabilized at 1.96 and 0.09, corresponding to 52% to 96% of the final OD in the control
288 group, respectively (Figure 6). Together, these results demonstrate that phage NL_ZS_3
289 was slightly more effective in reducing bacterial densities than the rest of the phages.

290 Despite *K. pneumoniae* ZS15 displaying a strong susceptibility to infection by all three
291 phages, phage NL_ZS_3 was better at suppressing resistance to host strain ZS15 over
292 phage NL_ZS_1 and NL_ZS_2. Bacteria are known to rapidly develop phage resistance
293 when subjected to predation by lytic phages in a laboratory medium (Labrie et al.,
294 2010). By screening phage resistance mutants, we attempted to better understand the
295 inhibition differences among each of the phage-amended cultures. Phage insensitive
296 mutants were isolated from phage lysate cultures during the incubation for the analysis

297 of changes in their susceptibility upon phage selection. Based on the results of spot test
298 assays, we observed that phage-amended cultures (ZS15+phage NL_ZS_1, ZS15+phage
299 NL_ZS_2, and ZS15+phage NL_ZS_3) were dominated by resistant non-mucoid clones
300 after 8 h of incubation, indicating conversion of mucoid *K. pneumoniae* strain ZS15 to
301 non-mucoid variants by consequence of selective pressure operated by phages (Table
302 3). However, in the ZS15+phage NL_ZS_3 cultures, heterogeneity in phage susceptibility
303 was observed (Table 3). Out of 30 *K. pneumoniae* ZS15 isolates, 2 (~6.7%) were fully
304 sensitive to phage NL_ZS_3 and displayed the hypermucoviscosity (HV) phenotype as
305 the parental strain ZS15, and partially sensitive (i.e., reduced phage susceptibly when
306 compared to the parental strain) subpopulations (~50%) were isolated as well and did
307 not revert back to the wild-type phenotype despite three rounds of purification.
308 Interestingly, 43.3% were fully resistant to phage NL_ZS_3, however, a small fraction
309 (~30%) of phage NL_ZS_3 resistant mutants reverted back to the parental phenotype
310 after three rounds of purification, suggesting different anti-phage mechanisms were
311 allowing coexistence of phage sensitive mutants and that their lytic phages could exist
312 between bacterial host ZS15 and phage NL_ZS_3. Since phage susceptibility was only
313 measured at 8 h, we do not know the dynamics of phenotype heterogeneity over time
314 or how long such persistence can last before heritage mutations dominate the entire
315 population.

316 **Anti-phage defense-mediated altered sensitivity to antibiotics**

317 Previous studies have shown that evolutionary phage-host interactions affect phage
318 resistance and antibiotic susceptibility both positively and negatively, and are highly

319 genotype-dependent in bacterial populations (Comeau et al., 2007;Chan et al.,
320 2016;Burmeister et al., 2020). We started to question whether phage-resistant mutants
321 changed their antibiotic susceptibilities via antagonistic coevolution between hosts and
322 parasites in LB broth. To investigate this further, we performed Vitek 2 assays for
323 antimicrobial susceptibility, testing phage-resistant mutants (ZS15-3R) and their
324 parental phage susceptible strains (ZS15). Interestingly, for tigecycline susceptibility
325 testing of carbapenem-resistant *K. pneumoniae* ZS15 strain, we noticed that strain ZS15
326 evolved resistance to phage NL_ZS_3, while simultaneously becoming more sensitive to
327 tigecycline with the minimum inhibitory concentration shifting from 8 μg/mL to 2
328 μg/mL. Unfortunately, we were unable to identify potential genes related to phage
329 selection and antibiotic sensitivity during the interactions between strain ZS15 and
330 phage NL_ZS_3. Further, comparative genomic sequence analyses are needed to
331 elucidate the underlying mechanisms.

332 **Discussion**

333 *Klebsiella pneumoniae* is a common nosocomial pathogen that causes difficult-to-treat
334 infections worldwide. The prevalence and distribution of bla_{KPC} gene in *K. pneumoniae* is
335 increasing, making carbapenem resistance isolates difficult to treat due to the lack of
336 effective and safe alternative options. Successful application of phage therapy in
337 treating *K. pneumoniae* caused infections requires a detailed understanding of the
338 phenotypic and genotypic diversity printers of *K. pneumoniae* pathogens as well as well-
339 characterized phages that covers host diversities. In this study, we characterized 3
340 phages and 22 *K. pneumoniae* strains, covering considerable temporal variability.

341 Further, *K. pneumoniae* strain ZS15 was selected for more detailed studies of phage lytic
342 potential and phage-host interactions.

343 **Diversity of *K. pneumoniae* ST11 isolates**

344 The clonal relationship between *K. pneumoniae* strains examined in the present study
345 belonged to ST11 irrespective of time or place of isolation. ST11 is among the most
346 important clinical dominant in Asia and South America and has been reported in
347 different regions worldwide since its emergence (Qi et al., 2011). In 2018, a fatal
348 outbreak of ST11 carbapenem-resistant hypervirulent *K. pneumoniae* in a Chinese
349 hospital has caused high mortality and morbidity (Gu et al., 2018;Yao et al., 2018).
350 Likely, ST258, single-locus variants of ST11 (the *tonB* allele distinguishes the two
351 sequence types), has emerged as an important cause of hospital death in the United
352 States and other countries, and is largely responsible for the global spread of KPC (Toth
353 et al., 2010). However, the molecular linage between ST11 and ST258 largely remains
354 unknown, recent comparative genomic analyses showed ST258 is a hybrid with ~80% of
355 the chromosome homology to ST11 strains, while the remaining 20% display high
356 similarity to the ST442 isolates (Chen et al., 2014). Despite MLST does not provide
357 sufficient discrimination for the 22 pathogenic isolates or resolve differences across
358 spatial and temporal sac ales, understanding the molecular evolutionary history of
359 bacterial isolates is an important step towards the development of diagnostic and
360 potential therapeutic strategies to combat infections caused by multidrug-resistant *K.*
361 *pneumoniae*.

362 Carbapenem resistance was seen among all *Klebsiella* isolates. Since carbapenem-
363 resistant *K. pneumoniae* (CRKp) are endemic to local hospitals, where colistin has been
364 largely used as the last treatment option to fight against these infections. Out of 22
365 strains, 2 isolates (strain ZS2 and ZS16) display resistance to colistin. Together, there 22
366 isolates could be regarded as a real superbug that could pose a major public health
367 challenge. There is currently little understanding of molecular mechanisms underlying
368 antibiotic resistance and its impact on virulence remain unclear, despite ~86% of strains
369 were confirmed to be carbapenemase gene positive. A recent sequence of complete *K.*
370 *pneumoniae* genomes showed that genes coding for resistance to antibiotics or
371 virulence factors is located in the plasmid. Moreover, the spread of these resistant
372 plasmids into the normal gut flora poses an even great public health threat. In order to
373 recapitulate the contents and diversity of the plasmids of genetically related *K.*
374 *pneumoniae* strains, it is important to track the spread of its plasmids between each
375 isolate. In our study, S1-PFGE showed four clusters of the CRKp producing strains that
376 corresponded to ST11, which demonstrates a high degree of genetic diversity. Future
377 work will seek to understand the dissemination of these plasmids and their potentials of
378 converting any *K. pneumoniae* strains with no existing antimicrobial resistance or
379 virulence determinants into CRKp strain immediately. Together, these results provide
380 important insights into relatively narrow phylogenetic and phenotypic groups of
381 bacteria, emphasizing the complexity for the development of alternatives to treat this
382 pathogen.

383 **Phage isolation and diversity**

384 Generally, phages are widespread and genetically diverse in almost all environments,
385 especially in sewage, known as a fertility source for many pathogens. The high
386 occurrence of *K. pneumoniae* phages in the collected samples (~72%) suggested the *K.*
387 *pneumoniae* phages are widespread in the local hospital sewage supply. The phages
388 isolated from the local hospital sewage displayed two distinguished host ranges when
389 tested against the collection of 22 *K. pneumoniae* isolates. Only 1 morphological family,
390 *Podoviridae*, was represented, and the phages ranged in genome size from 38 kb to 40
391 kb. Due to the limited sample numbers, we do not know to what extent these isolated
392 phages represent the true diversity and structure of local hospital sewage phage
393 communities. Further studies of viral metagenomics that are not dependent on cell
394 culture approaches are needed to expand our understanding of phage genomic diversity
395 from the evolutionary perspective and perhaps genetic exchanges in response to the
396 selection pressure from the bacterial host.

397 Phage NL_ZS_3 displayed a relatively broad host range, while phage NL_ZS_1 and phage
398 NL_ZS_2 shared identical relatively narrow host ranges, suggesting that phage NL_ZS_1
399 and phage NL_ZS_2 might use similar phage binding receptors to recognize bacterial
400 phage receptors in their susceptible hosts. This is interesting as bioinformatic analysis
401 showed that phage-binding receptors of phage NL_ZS_1 and phage NL_ZS_2 were
402 identical based on the amino acid sequence. The possible explanation for host range
403 difference could be phage NL_ZS_3 used a conservative apparatus as its phage
404 receptors, such as outer membrane proteins, lipopolysaccharides, flagella, or pili.
405 Moreover, several copies of genes encoding phage tails or tail fibers were present in the

406 phage NL_ZS_3, which opens the possibility that phage NL_ZS_3 may use a primary
407 receptor to initiate attachment but require a secondary cell surface receptor to
408 irreversibly bind to the bacterial host for injection, permitting more flexibility to develop
409 on a wider range of hosts. For example, the T4 phage uses its long tail fibers to
410 recognize lipopolysaccharide and the outer membrane protein C, present on the
411 bacterial surface (Tétart et al., 1996;Baslé et al., 2006). This reversible attachment
412 allows the phage to move along the surface and find a suitable site to inject its DNA.

413 **Phage-host interactions in strain ZS15**

414 Isolation and characterization of bacterial isolates during the LB broth experiments
415 confirmed the rapid development of phage resistance and subsequently dominated the
416 bacterial populations in the phage NL_ZS_1 and phage NL_ZS_2, which is regarded as a
417 significant barrier to the successful application of phage therapies (Koskella and
418 Meaden, 2013). Interestingly, in the current experiment with strain ZS15, phage NL_ZS_
419 3 exposures led to the rapid development of phenotypic diversity (i.e., resistant,
420 partially sensitive, and resistant) within a population that enables survival of fluctuating,
421 suggesting different anti-phage mechanisms were allowing coexistence of phage
422 sensitive mutants and that their lytic phages could exist. Since phage susceptibility was
423 only measured at 8 h, we do not know the dynamics of phenotype heterogeneity over
424 time or how long such persistence can last before heritage mutations dominate the
425 entire population. It is, therefore, crucial to characterize the phage-host interaction
426 regarding the phenotypic and genetic diversification in bacteria and phages prior to any

427 intended phage applications. The exact resistant mechanism by which strain ZS15 avoids
428 phages infection, however, remains to be discovered.

429 A common form of developing phage resistance for bacterial hosts is associated with
430 loss or altered structure of the receptors to block the potential phage adsorption in
431 order to avoid infection (Labrie et al., 2010). Such changes are directly linked to the key
432 step in recognition between phage receptor-binding proteins (RBP) located on tail
433 fibers, and phage receptors encoded on the susceptible bacterial host cell surface
434 (Bertozzi Silva et al., 2016). In general, the fitness costs resulting from receptor mutation
435 (i.e., motility, nutrient transport, or antimicrobial susceptibility) make the mutants
436 unable to compete with phage-susceptible strains in both environmental samples and
437 infection models, even in the presence of phage predation (Seed et al., 2012;Sumrall et
438 al., 2019). Understanding the evolutionary implication of phage-receptor interactions
439 will be beneficial for predicting how phages interact with their host, as phage receptor
440 mutation-mediated phenotypic variabilities may result in exopolysaccharide associated
441 fitness cost. Such characterization of phage resistance evolution will be used as a guide
442 for selecting proper phage targeting of specific receptors with a significant clinical
443 application. Our data reveal when phage resistance evolves, the resistant mutants
444 showed increased tigecycline sensitivity, despite the mechanism underlying potential is
445 not fully understood in this study.

446 Tigecycline, known as a tetracycline antibiotic, has shown the greatest antimicrobial
447 activity against CRKP. Genes e.g. *tet*(B), *tet*(A), *tet*(K), *tet*(M) and *tet*(S) coding for
448 multidrug efflux pumps are membrane-related proteins and can efflux tetracyclines

449 from the bacteria intracellularly, thus decreasing the MIC and subsequently allowing
450 protein synthesis without affecting cell viability (Linkevicius et al., 2016). Using
451 membrane-related proteins as a surface structure is one of the most common
452 components functioning as a phage receptor. Therefore, it makes sense that phage-
453 resistant defense strategies would confer a fitness cost for bacteria, i.e., becoming more
454 sensitive to certain antibiotics. For instance, in *P. aeruginosa*, phage OMKO1 evolved to
455 become less resistant to antibiotics. Likewise, in *E. coli*, the TolC protein evolved in a
456 variety of diverse cellular functions, including antibiotic efflux and phage TLS receptor
457 (Chan et al., 2016). However, unlike previous studies, the anti-phage TLS mediated TolC
458 mutation did not influence its role in antibiotic efflux. Overall, these results reveal that a
459 phage-host arm race can result in different outcomes in terms of antibiotic
460 susceptibilities, highlighting the diversity and complexity of host interactions within
461 bacterial populations.

462 **Potential applications of phage therapy**

463 Successful application of phage therapy requires collaboration between microbiology
464 and preclinical development; however, little is known about their alignment to guide
465 future development. Since the discovery of phages, many phages have been isolated
466 and identified as potential alternatives to antibiotics with different efficacy profiles.
467 Phage specificity is both a benefit and an obstacle for clinical trials, as phage receptor
468 diversity affects phage-host interaction. When the bacterial population is under phage
469 attack, only a small fraction of cells can survive these selective pressures, and those that
470 survive determine the fate of the population. Therefore, elucidating details of phage-

host interactions and how these would influence bacterial physiological heterogeneity is fundamental to the development of phage therapies. In this study, the three highlighted phages showed promising *in vitro* effects that perhaps these phages can be tamed for our benefits without negatively affecting their natural balance. The main limitation of this study is that only a small number of bacterial isolates and phages have been investigated. A large-scale study on the interactions between carbapenem-resistant K pneumoniae strains and phages covering a considerable spatial and temporal variability are essential for the successful application of phage-based pathogen control to fill our knowledge gap between *in vitro* and *in vivo* models.

Funding

This project was supported by the National Natural Science Foundation of China (NSFC) (No. 42006136), Shanghai Municipal Commission of Health (No.20204Y0336), and Shanghai Pujiang Talents Plan Project (No. 2020PJ054) to DT.

Acknowledgments

We thank Xiao Wang and Ruoyu Li for technical assistance. We thank all members from Zhu's lab for thoughtful discussions and grateful to Brett C. Gonzalez for proofreading the manuscript.

Declaration of competing interest

The authors declare no competing financial interests.

References

491 Abd El-Aziz, A.M., Elgaml, A., and Ali, Y.M. (2019). Bacteriophage Therapy Increases
492 Complement-Mediated Lysis of Bacteria and Enhances Bacterial Clearance After Acute
493 Lung Infection With Multidrug-Resistant Pseudomonas aeruginosa. *J Infect Dis* 219**,**
494 1439-1447.
495 Baslé, A., Rummel, G., Storici, P., Rosenbusch, J.P., and Schirmer, T.J.J.O.M.B. (2006). Crystal
496 structure of osmoporin OmpC from E. coli at 2.0 Å. 362**,** 933-942.
497 Bertozzi Silva, J., Storms, Z., and Sauvageau, D. (2016). Host receptors for bacteriophage
498 adsorption. *FEMS Microbiol Lett* 363.
499 Botelho, J., and Schulenburg, H. (2020). The Role of Integrative and Conjugative Elements in
500 Antibiotic Resistance Evolution. *Trends Microbiol*.
501 Burmeister, A.R., Fortier, A., Roush, C., Lessing, A.J., Bender, R.G., Barahman, R., Grant, R., Chan,
502 B.K., and Turner, P.E.J.P.O.T.N.a.O.S. (2020). Pleiotropy complicates a trade-off between
503 phage resistance and antibiotic resistance. 117**,** 11207-11216.
504 Bush, K., and Bradford, P.a.J.C.S.H.P.I.M. (2016). β-Lactams and β-lactamase inhibitors: an
505 overview. 6**,** a025247.
506 Cano, E.J., Caflisch, K.M., Bollyky, P.L., Van Belleghem, J.D., Patel, R., Fackler, J., Brownstein,
507 M.J., Horne, B.A., Biswas, B., and Henry, M.J.C.I.D. (2020). Phage Therapy for Limb-
508 threatening Prosthetic Knee Klebsiella pneumoniae Infection: Case Report and In Vitro
509 Characterization of Anti-biofilm Activity.
510 Capparelli, R., Parlato, M., Borriello, G., Salvatore, P., and Iannelli, D. (2007). Experimental phage
511 therapy against Staphylococcus aureus in mice. *Antimicrob Agents Chemother* 51**,** 2765-
512 2773.
513 Chan, B.K., Sistrom, M., Wertz, J.E., Kortright, K.E., Narayan, D., and Turner, P.E. (2016). Phage
514 selection restores antibiotic sensitivity in MDR Pseudomonas aeruginosa. *Sci Rep* 6**,**
515 26717.
516 Chen, L., Mathema, B., Pitout, J.D., Deleo, F.R., and Kreiswirth, B.N.J.M. (2014). Epidemic
517 Klebsiella pneumoniae ST258 is a hybrid strain. 5**,** e01355-01314.
518 Chibani-Chennoufi, S., Bruttin, A., Dillmann, M.L., and Brussow, H. (2004a). Phage-host
519 interaction: an ecological perspective. *J Bacteriol* 186**,** 3677-3686.
520 Chibani-Chennoufi, S., Sidoti, J., Bruttin, A., Kutter, E., Sarker, S., and Brussow, H. (2004b). In
521 vitro and in vivo bacteriolytic activities of Escherichia coli phages: implications for phage
522 therapy. *Antimicrob Agents Chemother* 48**,** 2558-2569.
523 Comeau, A.M., Tétart, F., Trojet, S.N., Prere, M.-F., and Krisch, H.J.P.O. (2007). Phage-antibiotic
524 synergy (PAS): β-lactam and quinolone antibiotics stimulate virulent phage growth. 2**,**
525 e799.
526 Dedrick, R.M., Guerrero-Bustamante, C.A., Garlena, R.A., Russell, D.A., Ford, K., Harris, K.,
527 Gilmour, K.C., Soothill, J., Jacobs-Sera, D., and Schooley, R.T. (2019). Engineered
528 bacteriophages for treatment of a patient with a disseminated drug-resistant
529 Mycobacterium abscessus. *Nature medicine* 25**,** 730.
530 Diancourt, L., Passet, V., Verhoef, J., Grimont, P.A., and Brisse, S. (2005). Multilocus sequence
531 typing of Klebsiella pneumoniae nosocomial isolates. *J Clin Microbiol* 43**,** 4178-4182.
532 Goren, M.G., Carmeli, Y., Schwaber, M.J., Chmelnitsky, I., Schechner, V., and Navon-Venezia, S.
533 (2010). Transfer of carbapenem-resistant plasmid from Klebsiella pneumoniae ST258 to
534 Escherichia coli in patient. *Emerg Infect Dis* 16**,** 1014-1017.
535 Gu, D., Dong, N., Zheng, Z., Lin, D., Huang, M., Wang, L., Chan, E.W.-C., Shu, L., Yu, J., and Zhang,
536 R.J.T.L.I.D. (2018). A fatal outbreak of ST11 carbapenem-resistant hypervirulent
537 Klebsiella pneumoniae in a Chinese hospital: a molecular epidemiological study. 18**,** 37-
538 46.

539 Hardiman, C.A., Weingarten, R.A., Conlan, S., Khil, P., Dekker, J.P., Mathers, A.J., Sheppard, A.E.,
540 Segre, J.A., and Frank, K.M. (2016). Horizontal Transfer of Carbapenemase-Encoding
541 Plasmids and Comparison with Hospital Epidemiology Data. *Antimicrob Agents*
542 *Chemother* 60**,** 4910-4919.
543 Hung, C.H., Kuo, C.F., Wang, C.H., Wu, C.M., and Tsao, N. (2011). Experimental phage therapy in
544 treating Klebsiella pneumoniae-mediated liver abscesses and bacteremia in mice.
545 *Antimicrob Agents Chemother* 55**,** 1358-1365.
546 Koskella, B., and Meaden, S. (2013). Understanding bacteriophage specificity in natural microbial
547 communities. *Viruses* 5**,** 806-823.
548 Kropinski, A.M., Mazzocco, A., Waddell, T.E., Lingohr, E., and Johnson, R.P. (2009). "Enumeration
549 of Bacteriophages by Double Agar Overlay Plaque Assay," in *Bacteriophages: Methods*
550 *and Protocols, Volume 1: Isolation, Characterization, and Interactions,* eds. M.R.J. Clokie
551 & A.M. Kropinski. (Totowa, NJ: Humana Press), 69-76.
552 Labrie, S.J., Samson, J.E., and Moineau, S. (2010). Bacteriophage resistance mechanisms. *Nat*
553 *Rev Microbiol* 8**,** 317-327.
554 Letkiewicz, S., Międzybrodzki, R., Fortuna, W., Weber-Dąbrowska, B., and Górski, A.J.F.M.
555 (2009). Eradication of Enterococcus faecalis by phage therapy in chronic bacterial
556 prostatitis—case report. 54**,** 457.
557 Linkevicius, M., Sandegren, L., and Andersson, D.I. (2016). Potential of Tetracycline Resistance
558 Proteins To Evolve Tigecycline Resistance. *Antimicrob Agents Chemother* 60**,** 789-796.
559 Mcvay, C.S., Velasquez, M., and Fralick, J.A. (2007). Phage therapy of Pseudomonas aeruginosa
560 infection in a mouse burn wound model. *Antimicrob Agents Chemother* 51**,** 1934-1938.
561 Pendleton, J.N., Gorman, S.P., and Gilmore, B.F. (2013). Clinical relevance of the ESKAPE
562 pathogens. *Expert Rev Anti Infect Ther* 11**,** 297-308.
563 Pitout, J.D., Nordmann, P., and Poirel, L. (2015). Carbapenemase-Producing Klebsiella
564 pneumoniae, a Key Pathogen Set for Global Nosocomial Dominance. *Antimicrob Agents*
565 *Chemother* 59**,** 5873-5884.
566 Pitout, J.D., Sanders, C.C., and Sanders Jr, W.E.J.T.a.J.O.M. (1997). Antimicrobial resistance with
567 focus on β-lactam resistance in gram-negative bacilli. 103**,** 51-59.
568 Qi, Y., Wei, Z., Ji, S., Du, X., Shen, P., and Yu, Y.J.J.O.a.C. (2011). ST11, the dominant clone of KPC-
569 producing Klebsiella pneumoniae in China. 66**,** 307-312.
570 Schooley, R.T., Biswas, B., Gill, J.J., Hernandez-Morales, A., Lancaster, J., Lessor, L., Barr, J.J.,
571 Reed, S.L., Rohwer, F., Benler, S.J.a.A., and Chemotherapy (2017). Development and use
572 of personalized bacteriophage-based therapeutic cocktails to treat a patient with a
573 disseminated resistant Acinetobacter baumannii infection. 61.
574 Seed, K.D., Faruque, S.M., Mekalanos, J.J., Calderwood, S.B., Qadri, F., and Camilli, A. (2012).
575 Phase variable O antigen biosynthetic genes control expression of the major protective
576 antigen and bacteriophage receptor in Vibrio cholerae O1. *PLoS Pathog* 8**,** e1002917.
577 Senchyna, F., Gaur, R.L., Sandlund, J., Truong, C., Tremintin, G., Kültz, D., Gomez, C.A.,
578 Tamburini, F.B., Andermann, T., Bhatt, A.J.D.M., and Disease, I. (2019). Diversity of
579 resistance mechanisms in carbapenem-resistant Enterobacteriaceae at a health care
580 system in Northern California, from 2013 to 2016. 93**,** 250-257.
581 Sulakvelidze, A., Alavidze, Z., and Morris, J.G., Jr. (2001). Bacteriophage therapy. *Antimicrob*
582 *Agents Chemother* 45**,** 649-659.
583 Sumrall, E.T., Shen, Y., Keller, A.P., Rismondo, J., Pavlou, M., Eugster, M.R., Boulos, S., Disson, O.,
584 Thouvenot, P., and Kilcher, S.J.P.P. (2019). Phage resistance at the cost of virulence:
585 Listeria monocytogenes serovar 4b requires galactosylated teichoic acids for InlB-
586 mediated invasion. 15**,** e1008032.

587 Suttle, C.A. (2005). Viruses in the sea. *Nature* 437**,** 356-361.
588 Tan, D., Gram, L., Middelboe, M.J.A., and Microbiology, E. (2014). Vibriophages and their
589 interactions with the fish pathogen Vibrio anguillarum. 80**,** 3128-3140.
590 Tétart, F., Repoila, F., Monod, C., and Krisch, H. (1996). "Bacteriophage T4 host range is
591 expanded by duplications of a small domain of the tail fiber adhesin". Elsevier).
592 Toth, A., Damjanova, I., Puskas, E., Jánvári, L., Farkas, M., Dobák, A., Böröcz, K., Paszti,
593 J.J.E.J.O.C.M., and Diseases, I. (2010). Emergence of a colistin-resistant KPC-2-producing
594 Klebsiella pneumoniae ST258 clone in Hungary. 29**,** 765-769.
595 Ventola, C.L. (2015). The antibiotic resistance crisis: part 1: causes and threats. *P T* 40**,** 277-283.
596 Yao, H., Qin, S., Chen, S., Shen, J., and Du, X.-D.J.T.L.I.D. (2018). Emergence of carbapenem-
597 resistant hypervirulent Klebsiella pneumoniae. 18**,** 25.

598

Fig. 1. Dendrogram generated by BioNumerics software (Version7.1, Applied Maths, St-Martens-Latem, Belgium) showing cluster results of molecular epidemiology S1-PFGE analysis of 21 *K. pneumoniae* isolates. Band-based similarity coefficients were calculated using Dice coefficient and unweighted pair group average method algorithm (UPGMA).

Fig. 2. Phage-host range assay of the 3 phages (columns) against the 22 *K. pneumoniae* isolates (rows). *Klebsiella pneumoniae* phages displayed broad and narrow host ranges. Black, grey and white indicate infection, weak infection and no plaque formation, respectively.

Fig. 3. Plaque images (up) and their corresponding TEM micrographs (below). Phages were stained with 2% sodium phosphotungstate and were found to have short small podophage morphology. Scale bar, 200 nm.

Fig. 4. The comparison of the whole genome sequences among three *K. pneumoniae* phages (NL_ZS_1, NL_ZS_2, and NL_ZS_3) with Easyfig using the BLASTN algorithm. Grey lines connect regions indicates nucleotide identity >66%, and are gradient-colored according to their similarity; darker shade of grey represents higher identify. The designations of the open reading frames of NL_ZS_1 are shown on the top.

Fig. 5. Phylogenetic tree was constructed based on the amino acid sequence of the larger terminase subunit of phages NL_ZS_1, NL_ZS_2, and NL_ZS_3 and phages sharing homology sequence identity retrieved from GenBank (https://www.ncbi.nlm.nih.gov/). The evolutionary history of 20 larger terminase subunit amino acid sequences were aligned and inferred using Neighbor Joining method and 1000 bootstrap replicates (CLC Genomics Workbench 8).

Fig. 6. Inhibition assay of phage NL_ZS_1, NL_ZS_2, and NL_ZS_3 in the treatment at an MOI of 0.1 and control without phage in cultures of *K. pneumoniae* ZS15. Optical density (OD600) was

measured at 1-h intervals over an 8-h incubation period. Error bars represent the standard deviations from all experiments, carried out in triplicate.

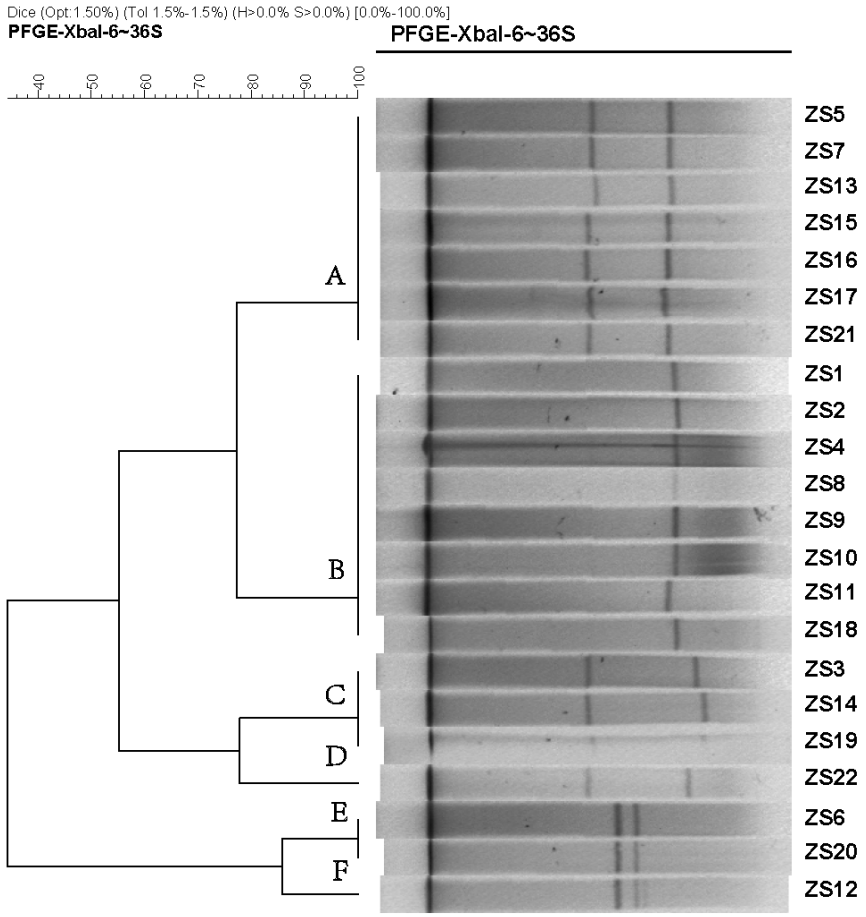
Dice (Opt:1.50%) (Tol 1.5%-1.5%) (H>0.0% S>0.0%) [0.0%-100.0%]
PFGE-XbaI-6~36S
PFGE-XbaI-6~36S
40
50
60
70
80
90
100
A
B
C
D
E
F
ZS5
ZS7
ZS13
ZS15
ZS16
ZS17
ZS21
ZS1
ZS2
ZS4
ZS8
ZS9
ZS10
ZS11
ZS18
ZS3
ZS14
ZS19
ZS22
ZS6
ZS20
ZS12

Strain	Phage		
	NL_ZS_1	NL_ZS_2	NL_ZS_3
ZS1			
ZS2			
ZS3			
ZS4			
ZS5			
ZS6			
ZS7			
ZS8			
ZS9			
ZS10			
ZS11			
ZS12			
ZS13			
ZS14			
ZS15			
ZS16			
ZS17			
ZS18			
ZS19			
ZS20			
ZS21			
ZS22			

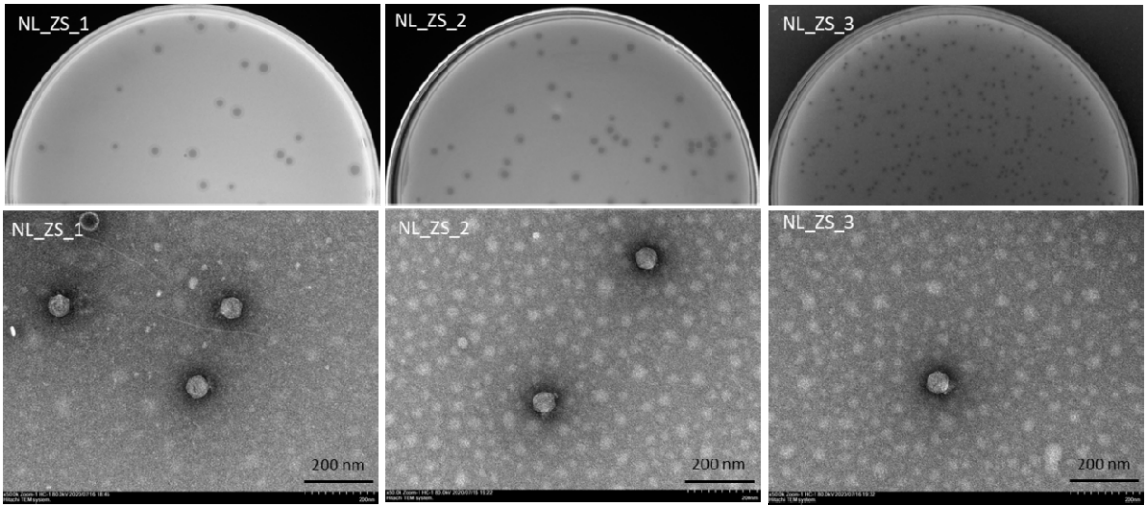
NL_ZS_1
NL_ZS_2
NL_ZS_3
NL_ZS_1
NL_ZS_2
NL_ZS_3
200 nm
200 nm
200 nm

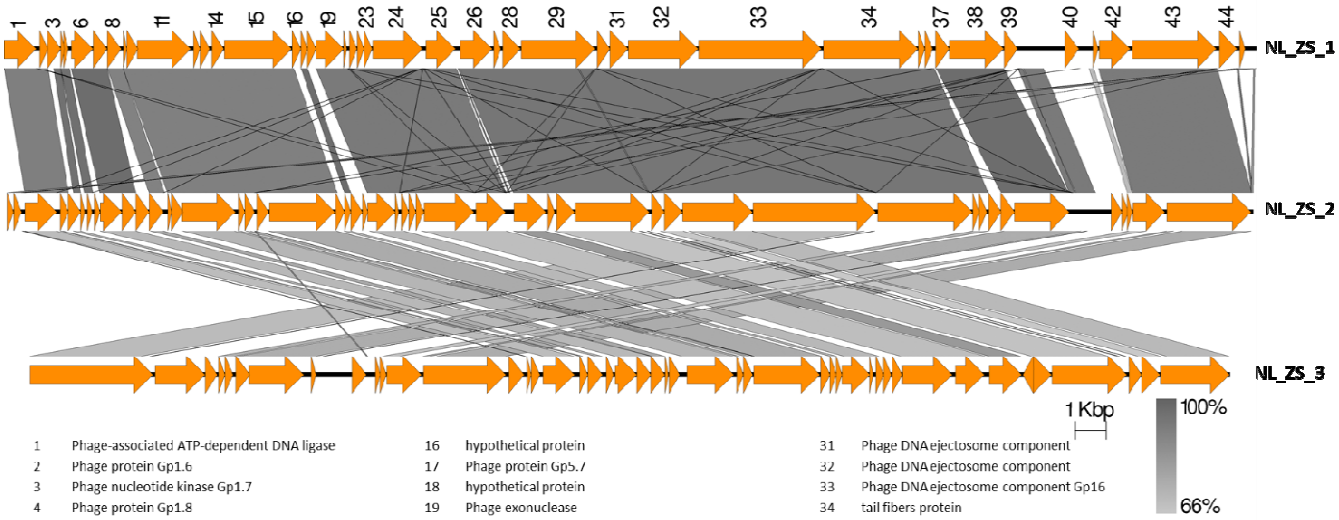

1	Phage-associated ATP-dependent DNA ligase	16	hypothetical protein	31	Phage DNA ejectosome component
2	Phage protein Gp1.6	17	Phage protein Gp5.7	32	Phage DNA ejectosome component
3	Phage nucleotide kinase Gp1.7	18	hypothetical protein	33	Phage DNA ejectosome component Gp16
4	Phage protein Gp1.8	19	Phage exonuclease	34	tail fibers protein
5	Phage protein Gp2	20	Phage protein Gp6.3	35	Phage holin, class II Gp17.5
6	Phage single-stranded DNA-binding proteinGp2.5	21	Phage protein Gp6.5	36	Phage terminase small subunit Gp18, DNApackaging
7	Phage endonuclease I	22	Phage virion protein Gp6.7	37	Phage Rz-like lysis protein Gp18.5
8	Phage endolysin	23	Phage virion assembly protein Gp7.3	38	Phage terminase large subunit Gp19, DNApackaging
9	Phage protein	24	Phage collar	39	Phage protein Gp7.8/Gp7.7 contains HNHendonuclease motif
10	Phage protein	25	Phage capsid assembly scaffolding protein Gp5	40	Phage S-adenosyl-L-methionine hydrolase
11	Phage primase/helicase protein Gp4A	26	Phage major capsid protein Gp10A	41	Phage protein
12	Phage protein Gp4.3	27	Phage protein	42	Phage serine/threonine kinase
13	Phage protein Gp4.5	28	Phage non-contractile tail tubular proteinGp11	43	Phage DNA-directed RNA polymerase
14	Phage protein Gp4.7	29	Phage non-contractile tail tubular proteinGp12	44	Phage protein
15	Phage DNA-directed DNA polymerase	30	Phage scaffold protein Gp13	45	Phage protein

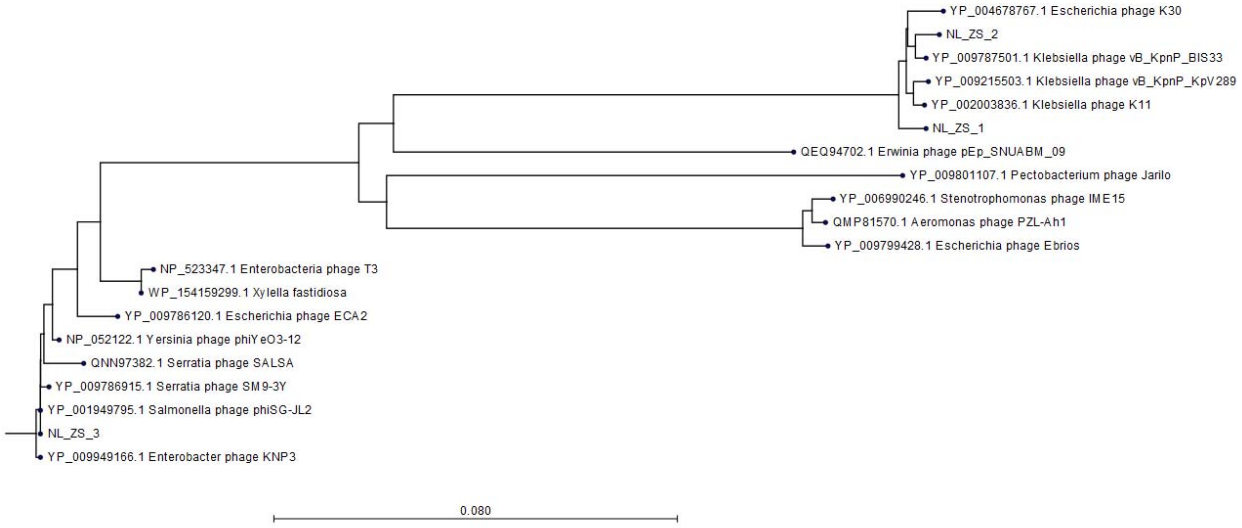
YP_004678767.1 Escherichia phage K30
NL_ZS_2
YP_009787501.1 Klebsiella phage vB_KpnP_BIS33
YP_009215503.1 Klebsiella phage vB_KpnP_KpV289
YP_002003836.1 Klebsiella phage K11
NL_ZS_1
QEQ94702.1 Erwinia phage pEp_SNUABM_09
YP_009801107.1 Pectobacterium phage Jarilo
YP_006990246.1 Stenotrophomonas phage IME15
QMP81570.1 Aeromonas phage PZL-Ah1
YP_009799428.1 Escherichia phage Ebrios
NP_523347.1 Enterobacteria phage T3
WP_154159299.1 Xylella fastidiosa
YP_009786120.1 Escherichia phage ECA2
NP_052122.1 Yersinia phage phiYeO3-12
QNN97382.1 Serratia phage SALSA
YP_009786915.1 Serratia phage SM9-3Y
YP_001949795.1 Salmonella phage phiSG-JL2
NL_ZS_3
YP_009949166.1 Enterobacter phage KNP3
0.080

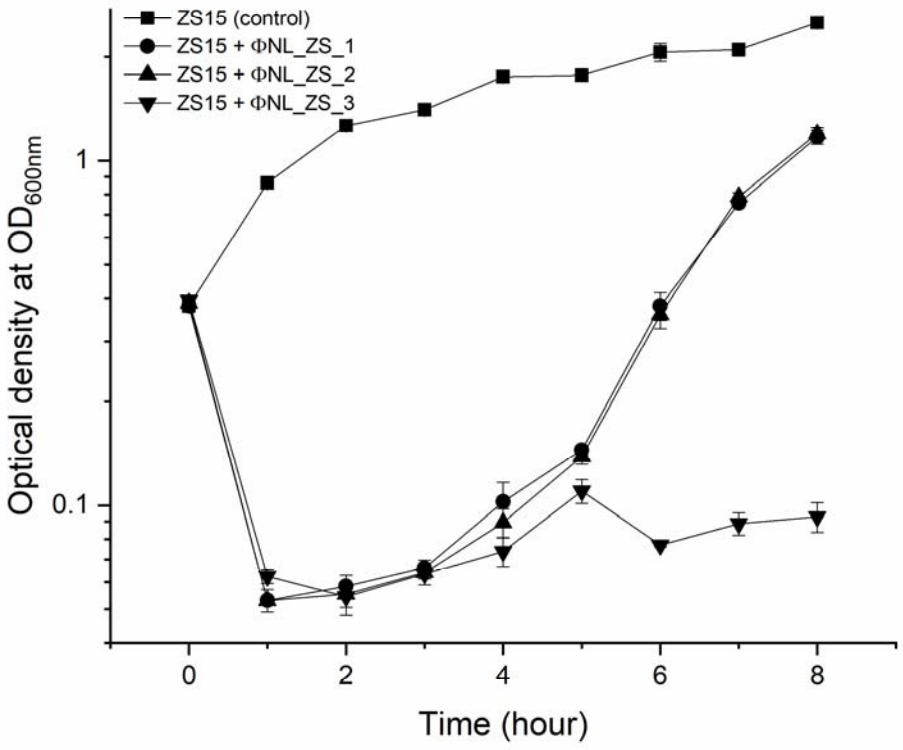
ZS15 (control)
ZS15 + ΦNL_ZS_1
ZS15 + ΦNL_ZS_2
ZS15 + ΦNL_ZS_3
Optical density at OD600nm
1
0.1
0
2
4
6
8
Time (hour)

Table 1. MLST types and antibiotic susceptibility profiles of the 22 *Klebsiella pneumoniae* isolates and their corresponding phage-resistant mutants. Antibiotic abbreviations: ticarcillin/clavulanic acid (TIM), piperacillin/tazobactam (TZP), ceftazidime (CAZ), cefoperazone (CPZ), cefepime (FEP), aztreonam (ATM), imipenem (IPM), meropenem (MEM), amikacin (AMK), tobramycin (TOB), ciprofloxacin (CIP), levofloxacin (LVX), doxycycline (DOX), minocycline (MIN), tigecycline (TGC), colistin (CST), trimethoprim-sulfamethoxazole (SXT).

Table 2. Morphological and genomic characterization of phages isolated from the local hospital sewage.

Table 3. Phage susceptibility properties of *K. pneumoniae* ZS15 isolates obtained from cultures enriched with the phages. “Resistant” indicates that isolates were not susceptible to phage infection in the spot test. “Partially sensitive” indicates that isolates had a reduced susceptibility to the phage. “Sensitive” indicates that isolates were fully sensitive to the phage.

			Minimum inhibitory concentration (μg/mL)																
Strain	MLST	bla_{KPC}	TIM	TZP	CAZ	CPZ	FEP	ATM	IMP	MEM	AMK	TOB	CIP	LVX	DOX	MIN	TGC	CST	SXT
ZS1	ST11	Yes	≥128	≥128	≥64	≥64	≥32	≥64	≥16	≥16	≥64	≥16	≥4	≥8	2	4	≤0.5	≤0.5	≤20
ZS2	ST11	Yes	≥128	≥128	≥64	32	≥32	≥64	≥16	≥16	4	8	≥4	≥8	2	8	1	≥16	≤20
ZS3	ST11	No	≥128	≥128	≥64	≥64	≥32	≥64	1	1	≥64	≥16	≥4	≥8	4	≥16	2	≤0.5	≤20
ZS4	ST11	Yes	≥128	≥128	32	≥64	≥32	≥64	0.5	≤0.25	≥64	≥16	≥4	≥8	2	8	1	≤0.5	≤20
ZS5	ST11	Yes	≥128	≥128	≥64	≥64	≥32	≥64	≥16	≥16	4	≤1	≥4	≥8	8	≥16	4	≤0.5	≤20
ZS6	ST11	Yes	≥128	≥128	≥64	≥64	≥32	≥64	≥16	≥16	≥64	≥16	≥4	≥8	1	2	≤0.5	≤0.5	≤20
ZS7	ST11	Yes	≥128	≥128	≥64	≥64	≥32	≥64	≥16	≥16	4	≤1	≥4	≥8	≥16	≥16	≥8	≤0.5	≤20
ZS8	ST11	Yes	≥128	≥128	≥64	≥64	≥32	≥64	≥16	≥16	≥64	≥16	≥4	≥8	4	8	2	≤0.5	≤20
ZS9	ST11	Yes	≥128	≥128	≥64	≥64	≥32	≥64	≥16	≥16	≥64	≥16	≥4	≥8	4	8	2	≤0.5	≤20
ZS10	ST11	Yes	≥128	≥128	≥64	≥64	≥32	≥64	≥16	≥16	≥64	≥16	≥4	≥8	≥16	≥16	4	4	≥320
ZS11	ST11	Yes	≥128	≥128	≥64	≥64	≥32	≥64	≥16	≥16	≥64	≥16	≥4	≥8	2	8	2	≤0.5	≤20
ZS12	ST11	Yes	≥128	≥128	≥64	≥64	≥32	≥64	≥16	≥16	≥64	≥16	≥4	≥8	2	8	1	≤0.5	≤20
ZS13	ST11	Yes	≥128	≥128	≥64	≥64	≥32	≥64	≥16	≥16	≥64	≥16	≥4	≥8	2	8	≤0.5	≤0.5	≤20
ZS14	ST11	No	≥128	≥128	32	≥64	≥32	≥64	1	0.5	≥64	≥16	≥4	≥8	2	8	≤0.5	≤0.5	≤20
ZS15	ST11	Yes	≥128	≥128	≥64	≥64	≥32	≥64	≥16	≥16	≥64	≥16	≥4	≥8	2	8	8	≤0.5	≤20
ZS16	ST11	Yes	≥128	≥128	≥64	≥64	≥32	≥64	≥16	≥16	≥64	≥16	≥4	≥8	4	≥16	2	≥16	≤20
ZS17	ST11	Yes	≥128	≥128	≥64	≥64	≥32	≥64	≥16	≥16	≥64	≥16	≥4	≥8	4	8	1	≤0.5	≤20
ZS18	ST11	Yes	≥128	≥128	≥64	32	≥32	≥64	≥16	8	8	≤1	≥4	≥8	≤0.5	2	≤0.5	≤0.5	≤20
ZS19	ST11	No	≥128	≥128	8	≥64	≥32	≥64	≤0.25	≤0.25	≥64	≥16	≥4	≥8	2	4	≤0.5	≤0.5	≤20
ZS20	ST11	Yes	≥128	≥128	≥64	≥64	≥32	≥64	≥16	≥16	≥64	≥16	≥4	≥8	1	4	≤0.5	≤0.5	≤20
ZS21	ST11	Yes	≥128	≥128	≥64	≥64	≥32	≥64	≥16	≥16	≥64	≥16	≥4	≥8	1	4	≤0.5	≤0.5	≤20
ZS22	ST11	Yes	≥128	≥128	≥64	≥64	≥32	≥64	≥16	≥16	≥64	≥16	≥4	≥8	1	2	≤0.5	≤0.5	≤20

Phage	Family	Host	Head diam (nm)	Head length (nm)	Tail diam (nm)	Tail length (nm)	Genome size (bp)	GC%	Genome type	Predicted genes	Source
NL_ZS_1	Podoviridae	ZS15	63	58	13	14	40,428	53	dsDNA	45	Sewage
NL_ZS_2	Podoviridae	ZS15	58	63	13	9	40,222	52.8	dsDNA	49	Sewage
NL_ZS_3	Podoviridae	ZS15	63	63	13	11	38,741	50.7	dsDNA	46	Sewage

Percentage of phage susceptibility properties of *K. pneumoniae* ZS15 isolates (%)

Phage	Resistant	Partially sensitive	Sensitive
NL_ZS_1	100%	0	0
NL_ZS_2	100%	0	0
NL_ZS_3	43.3%	50%	6.7%